ELSEVIER

Biochimica et Biophysica Acta 1365 (1998) 453–463

BIOCHIMICA ET BIOPHYSICA ACTA
BBA

Oxygen permeability of thylakoid membranes: electron paramagnetic resonance spin labeling study

Agnieszka Ligeza [a,b], Alexander N. Tikhonov [a,c], James S. Hyde [b], Witold K. Subczynski [a,b,*]

[a] *Biophysics Department, Institute of Molecular Biology, Jagiellonian University, Al. Mickiewicza 3, 31-120 Krakow, Poland*
[b] *Biophysics Research Institute, Medical College of Wisconsin, Milwaukee, WI, USA*
[c] *Department of Biophysics, Faculty of Physics, M.V. Lomonosov Moscow State University, Moscow, 119899, Russian Federation*

Received 6 April 1998; accepted 7 April 1998

Abstract

Oxygen transport in thylakoid membranes of spinach chloroplasts (*Spinacia oleracea*) has been studied by observing the collisions of molecular oxygen with spin labels, using line broadening electron paramagnetic resonance (EPR) spectroscopy. Stearic acid spin labels were used to probe the local oxygen diffusion–concentration product. The free radical moiety was located at various distances from the membrane surface, and collision rates were estimated from linewidths of the EPR spectra measured in the presence and absence of molecular oxygen. The profile of the local oxygen diffusion–concentration product across the membrane determined at 20°C demonstrates that this product, at all membrane locations, is higher than the value measured in water. From the profile of the oxygen diffusion–concentration product, the membrane oxygen permeability coefficient has been estimated using the procedure developed earlier (W.K. Subczynski, J.S. Hyde, A. Kusumi, Proc. Natl. Acad. Sci. USA 86 (1989) 4474–4478). At 20°C, the oxygen permeability coefficient for the lipid portion of the thylakoid membrane was found to be 39.5 cm s^{-1}. This value is 20% higher than the oxygen permeability coefficient of a water layer of the same thickness as the thylakoid membrane. The high permeability coefficient implies that the oxygen concentration difference across the thylakoid membrane generated under the illumination of the leaf by saturating actinic light is negligible, smaller than 1 μM.

Keywords: Thylakoid membrane; Oxygen permeability; Spin label

1. Introduction

Oxygen is actively involved in light-induced redox processes in plants. The chloroplast electron transport chain (ETC) leads to release of oxygen through the water-splitting complex of photosystem 2 (PS2), and oxygen consumption at the acceptor side of photosystem 1 (PS1) [1]. There is experimental evidence that oxygen plays an essential role in the regulation of electron transport in native chloroplasts: (1) oxygen acts as the mediator of pseudocyclic electron

Abbreviations: PS1, Photosystem 1; PS2, Photosystem 2; ETC, electron transport chain; EPR, electron paramagnetic resonance; 5-, 9-, 12- and 16-SASL, 5-, 9-, 12- and 16-doxylstearic acid spin label; DMPC, dimyristoylphosphatidylcholine; MGDG, monogalactosyldiacylglycerol; DGDG, digalactosyldiacylglycerol

* Corresponding author. Fax: +48 (12) 633-6907; E-mail: subczyn@mol.uj.edu.pl

0005-2728/98/$19.00
PII: S0005-2728(98)00098-X

transport [2,3]; (2) oxygen is involved in chloroplast photorespiration [4]; (3) the concentration of oxygen in chloroplasts controls ATP formation [3–8]; and (4) the presence of oxygen appears to be the obligatory condition for normal functioning of chloroplast ETC in situ [2,9]. These circumstances suggest that light-induced modulation of oxygen concentration in the interior of a leaf might be an essential factor in the regulation of chloroplast metabolism in vivo. In particular, in our previous work [10] we have demonstrated the correlation between the kinetics of the redox transients of PS1 reaction center P_{700} and the light-induced changes in the oxygen concentration inside a leaf.

An oxygen concentration difference across the thylakoid membrane might occur because of the asymmetrical arrangement of ETC components. A water-splitting complex of PS2 is exposed to the thylakoid interior, while the oxygen-reducing components of ETC are located at the outer side of the thylakoid membrane or in the bulk phase of chloroplast stroma. Therefore, oxygen evolved by the PS2 water-splitting complex diffuses through the thylakoid membrane from the internal side of thylakoid to the external bulk phase (stroma). The high protein content and the presence of boundary lipids may provide a barrier to oxygen transport through the thylakoid membrane. If the membrane permeability for oxygen is rather small, one could expect the appearance of a steady-state oxygen concentration difference across the thylakoid membrane. We cannot rule out the possibility that oxygen produced by the water-splitting complex buried deeply in the PS2 can be released to the stroma side of the thylakoid membrane via a specific path (channel) in this protein complex. This hypothesis was already raised for channeling of oxygen into the respiratory enzyme [11].

One of the questions concerning the regulatory role of oxygen is whether the local concentrations of oxygen in different compartments of chloroplast increase to such a high level that the redox states of ETC components could be affected, and thus influence electron flow. Under certain conditions, a light-induced, supersaturated oxygen concentration can be created in the aqueous solution surrounding cyanobacteria, which leads to photo-oxidative damage to both photosynthesis and respiration [12]. High local concentrations of oxygen inside chloroplasts can also stimulate the formation of active forms of oxygen (superoxide anion radicals, hydrogen peroxide) which should lead to the photodestruction of pigments and degradation of proteins [13–15]. However, due to the subcompartmentalization of a chloroplast, it is practically impossible to measure directly an oxygen concentration difference across the thylakoid membrane or to determine a local concentration of oxygen in a particular chloroplast compartment. Conventional methods for oxygen monitoring provide only an averaged picture of oxygen production or consumption. Indeed, the use of a macroscopic Clark electrode cannot help in measuring oxygen concentration in the interior of the leaf. An application of microscopic paramagnetic oxygen-sensitive probes (see, e.g. [10,16,17]) appears to be promising for monitoring the modulation of the oxygen level inside a leaf. However, the lack of information on partitioning of the microscopic probe between the thylakoid lumen, membranes and stroma impacts negatively on efforts to measure the local concentrations of oxygen in different compartments of a functioning chloroplast.

An answer to the question about possible oxygen gradients in chloroplasts is tightly associated with oxygen permeability through the thylakoid membrane. In this work, we have estimated the oxygen permeability coefficient for the thylakoid membrane from the profile of the oxygen diffusion–concentration product across the membrane, using the procedure developed earlier [18,19]. This profile was obtained by observing the oxygen broadening of the electron paramagnetic resonance (EPR) spectrum of lipid-soluble spin labels located at various distances from the membrane surface, which is determined by the product of the local oxygen concentration and the local oxygen diffusion coefficient [20,21]. Having determined the thylakoid membrane permeability coefficient for oxygen, we evaluated the oxygen concentration difference that could be generated across the thylakoid membrane during chloroplast illumination. An elementary estimate showed that under steady-state physiological conditions, the oxygen concentration difference across the thylakoid membrane should be negligible.

2. Theoretical background

Previously, we have shown that spin label oximetry is a quantitative method that allows the calculation of the oxygen diffusion–concentration product and oxygen permeability across the membrane [18,19,22]. We demonstrated [20,21] that in water every collision of oxygen with a nitroxide radical leads to an observable-event–line-broadening of the EPR spectrum. Since this method works so well in water with its low viscosity, it is almost certain to work in higher viscosity solvents such as oils and membranes (see also [23,24] for further discussion). These results allow us to connect the Smoluchowski equation for colliding molecules,

$$\omega = 4\pi pRD(x)C(x) \quad (1)$$

with oxygen-induced line broadening of the EPR spin label spectrum, expressed in frequency units [25,26]:

$$\omega = \frac{\sqrt{3}}{2}\gamma\Delta H_{pp}(x). \quad (2)$$

In Eq. 1, $C(x)$ is the local oxygen concentration at 1 atm partial pressure of oxygen, R is the interaction distance between oxygen and nitroxide radical, and p is the probability that an observable event is recorded when a collision takes place. The Smoluchowski equation for the bimolecular collision rate of dissolved oxygen molecules with various spin labels yields values for the diffusion coefficient of oxygen in water that are in agreement with published values obtained by conventional methods [20,21]. The most significant aspect of that agreement is that a Heisenburg exchange at an interaction distance of 4.5 Å occurs with a probability close to 1 for each encounter. The exchange integral between spin label and oxygen is sufficiently strong to result in a measurable event on every collision, even though the translational correlation time is as short as 10^{-11} s. Also, our evaluations in hydrophobic hydrocarbon solvents give similar values of R and p [20,23]. It is also assumed that the diffusion coefficient of oxygen, $D(x)$, is much higher than the diffusion coefficient of the spin label. In fluid-phase membranes, the average diffusion coefficient of oxygen is $1.5–1.8\times10^{-5}$ cm^2 s^{-1} [24,27] while that of 16-SASL is 5.8×10^{-8} cm^2 s^{-1} [28]. In water, however, this difference is not as great. At 20°C, the diffusion coefficient of oxygen equals 2×10^{-5} cm^2 s^{-1} [29] and for TEMPONE (the nitroxide spin label of the size of free-radical moiety of SASL) equals 0.6×10^{-5} cm^2 s^{-1} [30]. The diffusion coefficient of SASL in water is not available, but should be smaller than that of TEMPONE. We can estimate, however, that without correction the final result is underestimated by not more than 20%.

$\Delta H_{pp}(x)$ is the oxygen-induced peak-to-peak line broadening at 1 atm partial pressure and γ is the magnetogyric ratio of the electron. The value of $\Delta H_{pp}(x)$ can been determined directly from the experiment as:

$$\Delta H_{pp}(x) = H_{pp}(x, O_2) - H_{pp}(x, N_2), \quad (3)$$

where $H_{pp}(x,O_2)$ and $H_{pp}(x,N_2)$ are the peak-to-peak linewidths of the central component of the EPR spectrum of nitroxide spin labels for samples equilibrated with oxygen or nitrogen, respectively, at 1 atm pressure. Eq. 2 is appropriate, in principle, if the line shape of the EPR signal in the absence of oxygen is Lorentzian. No specific measurements of line shapes were made, and for more accurate measurements such a procedure would be appropriate. Our measurements were performed for the central line of SASL, which is Lorentzian in shape over the widest range of experimental conditions. Also, CW saturation curves of SASLs in water and in membranes indicate a high degree of homogeneity of this line. The variable x indicates the 'depth' (the position of the nitroxide moiety) in the membrane. Thus, the measurement of $\Delta H_{pp}(x)$ yields the product of the local translational diffusion coefficient, $D(x)$, and the local concentration of oxygen, $C(x)$, at depth x in the membrane. In our previous paper [31], we reported the existence of vertical fluctuations of the nitroxide moiety of SASL towards the polar surface of the lipid bilayer. Measurements were made of bimolecular collision rates between moieties at different locations on the alkyl chain. Information on the time-average depth, however, is not available. Fortunately, neutron diffraction measurements in deuterated phosphatidylcholine membranes [32] show that the average position of the carbon atoms in the alkyl chain can be determined with an accuracy of ± 1.5 Å. It is also reported that the width of the label distribution is found to increase at the end of the

chain. These measurements indicate that most of the time, the carbon atom (in our case, the nitroxide moiety) stays at the position determined by Zaccai et al. [32]. In our further calculations, we assume that the nitroxide moiety of SASL is located at the mean depth of a given carbon in the 1- and 2-chain in the phospholipid. The oxygen translational correlation time ($\sim 10^{-11}$ s) is much shorter than the spin label rotational correlation time ($\sim 10^{-9}$ s), and SASL rotation does not affect the measured oxygen diffusion–concentration product in membranes.

The oxygen permeability coefficient across the membrane, P_m, can be determined from the membrane profile of the oxygen diffusion–concentration product, $D(x)C(x)$, based on the theory of Diamond and Katz [33] and a procedure developed by Subczynski et al. [18]. It is necessary to make an integration of $(D(x)C(x))^{-1}$, which is a measure of the resistance to oxygen permeation, over the entire thickness, h, of the membrane. The product $D(x)C(x)$ is connected with the oxygen-induced line broadening, $\Delta H_{pp}(x)$, through Eqs. 1 and 2. According to [19], the final expression for P_m has the following form:

$$P_m(\mathrm{EPR}) = \left(\frac{8\pi pR}{\sqrt{3}\gamma} C_W \int_0^h \frac{dx}{\Delta H_{pp}(x)}\right)^{-1}. \quad (4)$$

Here, C_W is the oxygen concentration in water equilibrated with 1 atm partial pressure of oxygen and 'EPR' indicates that P_m is determined based on EPR measurements.

The oxygen permeability across the water layer of the same thickness as the membrane can be determined as:

$$P_W(\mathrm{EPR}) = \left(\frac{8\pi pR}{\sqrt{3}\gamma} C_W \frac{h}{\Delta H_{pp}(\mathrm{water})}\right)^{-1}, \quad (5)$$

where ΔH_{pp}(water) is the EPR signal broadening induced by the equilibration of a water sample containing spin label with 1 atm pressure of oxygen. In our experiments, ΔH_{pp}(water) was determined using 2×10^{-4} M solution of 16-doxylstearic acid spin label. Other SASLs exhibit the same oxygen-induced line broadening [19], but are less soluble in water.

Since the product pR is remarkably independent of solvent viscosity, hydrophobicity, and spin-label species [20,21,23,24], the relative value of oxygen permeability across the membrane, $P_m(\mathrm{EPR})/P_W(\mathrm{EPR})$, which does not contain parameters p and R, can be determined from Eqs. 4 and 5. Thus, it becomes possible to overcome uncertainties in the values of p and R. To determine the absolute value of the oxygen permeability across the membrane, P_m, the oxygen permeability coefficient P_W for a water layer of the thickness h, has been used. It can be determined independent of P_W(EPR) from the macroscopic diffusion coefficient of oxygen in water D_W [29] according to the equation:

$$P_W = D_W/h. \quad (6)$$

Thus, the absolute value for the oxygen permeability coefficient across the membrane is given by Eq. 7.

$$P_m = \frac{P_m(\mathrm{EPR})}{P_W(\mathrm{EPR})} P_W. \quad (7)$$

These equations are valid if oxygen diffusion is isotropic. It has been previously shown, using lipid-soluble spin labels with a different orientation of the π-orbital of the nitroxide radical relative to the membrane normal, that oxygen diffusion in the pure fluid-phase dimyristoylphosphatidylcholine (DMPC) membranes is almost isotropic [34]. This has also been concluded from fluorescence measurements of oxygen diffusion through membranes [27]. A molecular dynamics simulation of translational diffusion of NO in the hydrocarbon region of the DMPC bilayer led to the same conclusion [35]. Calculated average coefficients of the NO translational diffusion in both lateral and transverse directions appear to be the same. Similarly, the lateral diffusion profile of water molecules in a DMPC bilayer obtained from molecular dynamics simulation was very similar to the transverse profile [36], which indicates that on the local scale of diffusion the membrane looks essentially isotropic. To our knowledge no simulation of oxygen diffusion in the lipid bilayer has been performed, but because of similar physical properties, the diffusion of NO should closely resemble oxygen diffusion [37,38]. Also it is argued that the mechanism of diffusion of small molecules (MW < 50) in membranes is the same [22], so conclusions from NO and H_2O diffusion can be extended to oxygen diffusion. Thus, experimental results and computer simulations indicate that molecular oxygen diffuses iso-

tropically in the hydrophobic hydrocarbon region of the membrane.

3. Materials and methods

3.1. Reagents

5-, 9-, 12- and 16-doxylstearic acid spin labels (5-, 9-, 12- and 16-SASL) were obtained from Molecular Probes, (Eugene, OR). Other reagents were obtained from Sigma (St. Louis, MO).

3.2. Preparation of thylakoid membranes

Thylakoid membranes were isolated from spinach leaves (*Spinacia oleracea*) according to the method described earlier [39]. Deveined leaves were homogenized in ice-cold 50 mM HEPES buffer, pH 7.6, containing 5 mM $MgCl_2$, 50 mM NaCl and 0.3 M mannitol as osmoticum. The homogenate was filtered through four layers of cheesecloth and centrifuged for 4 min at $600\times g$. The supernatant was centrifuged for 10 min at $1500\times g$ and the resulting pellet was suspended for 20 min in osmotic shock buffer (10 mM HEPES, pH 7.6, 5 mM $MgCl_2$ and 10 mM NaCl). Then the suspension was centrifuged for 10 min at $2500\times g$ and the pellet of thylakoid membranes was suspended in homogenization buffer at the concentration of chlorophyll (about 1 mg/ml). All manipulations of thylakoid membranes, including EPR measurements, were performed in dark or dim light to prevent light-induced redox transformation of the spin labels.

3.3. Spin labeling of thylakoid membranes

A spin-label film was prepared on the bottom of a 10-ml beaker by drying 50 μl of the 1 mM chloroform solution of *n*-SASL. Then the 0.5 ml suspension of thylakoid membranes was added to the beaker and shaken for 30 min at room temperature. After shaking, the sample was placed into an Eppendorf tube and centrifuged for 15 min at 4°C. The thick membrane suspension was transferred to a thin-wall gas-permeable capillary (0.7 mm i.d.) made of the methylpentene polymer, TPX [23]. This plastic is permeable to oxygen and nitrogen, but is substantially impermeable to water. Our control measurements demonstrated that this incubation time was sufficient to incorporate all spin-label molecules. Based on data from the literature and our own observations, we assumed that SASLs are distributed symmetrically in the membrane, i.e. with the carboxyl groups facing either the stromal or the lumenal surface of the thylakoid membrane. It was demonstrated ([40] and citations therein) that SASLs, when added to the suspension of intact cells, are located in all cellular membranes and that SASLs are in rapid equilibrium throughout the membranous system of the cell. It was also shown that the flip-flop of fatty acids and long-chain nitroxide esters in phospholipid bilayers is fast [41,42]. The spin-labeled suspension of thylakoid membranes was immediately used for EPR measurements.

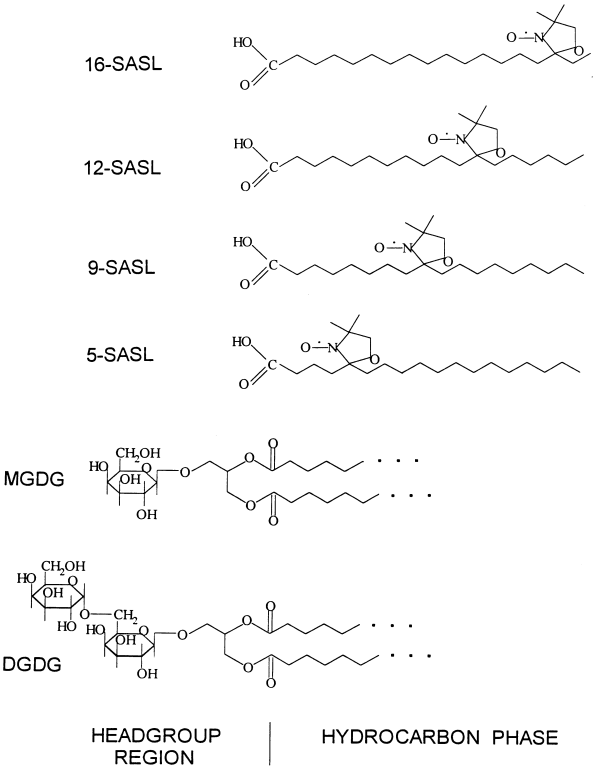

Fig. 1. Chemical structures of monogalactosyldiacylglycerol (MGDG), digalactosyldiacylglycerol (DGDG), and spin labels used in this work. Spin labels are intercalated in the membrane with the hydrophilic part (left-hand side) in the polar headgroup region of the membrane. The locations of the nitroxide moiety in the stearic acid molecule are shown. Galactolipids are major components of the lipid portion of thylakoid membranes (see also Table 1, footnotes).

3.4. EPR measurements

The TPX plastic capillary was positioned inside the EPR dewar insert and EPR measurements were carried out with a Varian E-109 X-band spectrometer. To determine the extent of oxygen-induced line broadening, the peak-to-peak linewidth of the central component of the spin-label EPR spectrum was measured first for the sample equilibrated with nitrogen, and then for the sample equilibrated with oxygen. Equilibrations with nitrogen and oxygen, as well as EPR measurements, were performed at 20°C. The microwave power was 1 mW, scan range 10 G, and modulation amplitude about five times smaller than the linewidth. Every point was repeated several times.

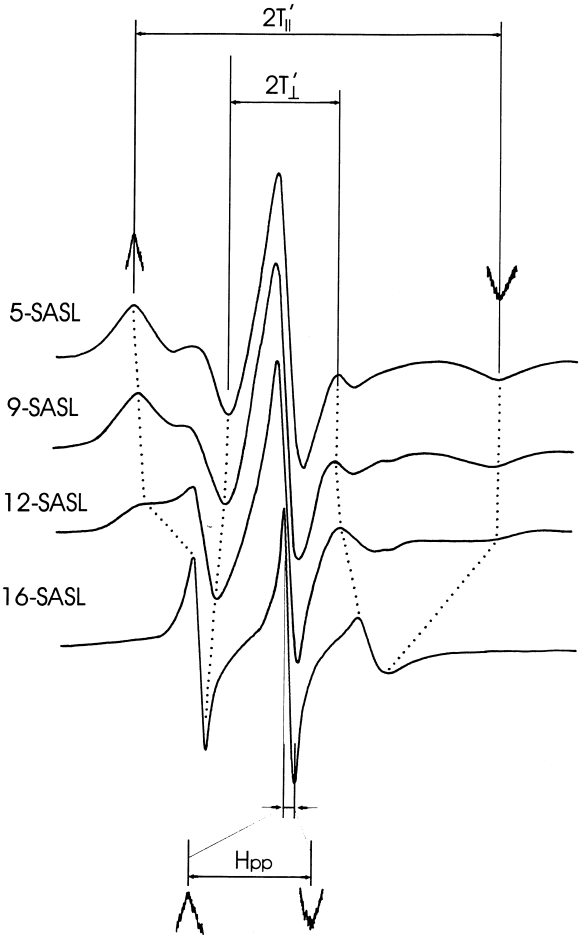

Fig. 2. EPR spectra of doxylstearic acid spin labels (5-, 9-, 12- and 16-SASL) in thylakoid membranes recorded at 20°C for samples equilibrated with nitrogen. The measured parameters are indicated. The outer wings were also magnified by recording at 10 times the receiver gain. Peak-to-peak central linewidths were recorded with expanded abscissa (magnetic field scan range by a factor of 10).

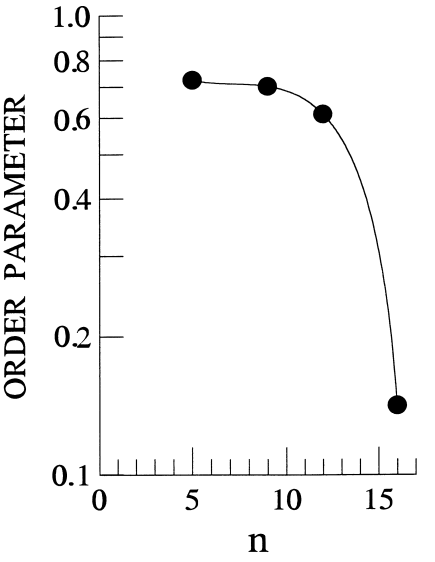

Fig. 3. Order parameter S of SASL in thylakoid membranes at 20°C (measured as a function of nitroxide position (n) along the hydrocarbon chain in stearic acid).

4. Results and discussion

4.1. EPR spectra of stearic acid spin labels in thylakoid membranes

Fig. 1 shows the structures of the lipid-soluble spin labels (derivatives of stearic acid) used in this work together with the structures of the main lipid components of thylakoid membrane monogalactosyldiacylglycerol (MGDG) and digalactosyldiacylglycerol (DGDG) (see also Table 1, more details in footnotes). When dissolved in thylakoid membranes, these molecules give EPR spectra (Fig. 2) that are typical of spectra of SASLs located in a hydrophobic membrane environment. Spectra in Fig. 2 show no evidence of signals that might come from nitroxide radicals located in aqueous surroundings. Since no 'hydrophobic' or 'polar' signals are superimposed, the linewidth of the central component of the EPR spin-label spectrum can be used as the most sensitive parameter to evaluate the broadening effect of oxygen dissolved in the lipid bilayer. The mobility of

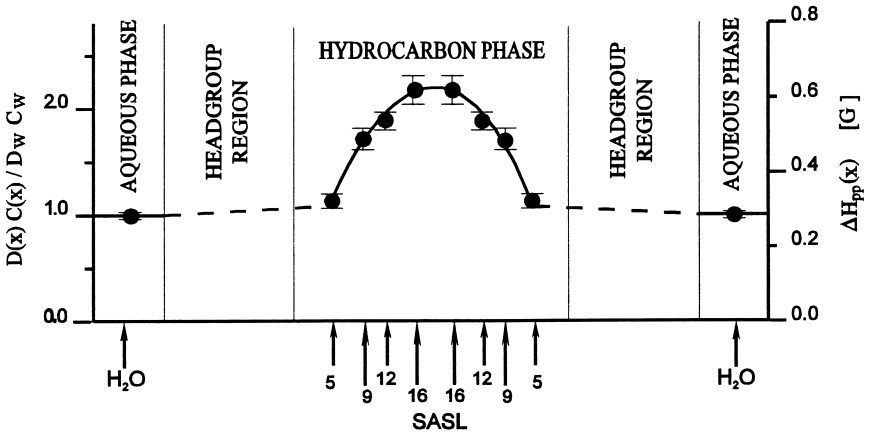

Fig. 4. Profile of the relative oxygen diffusion–concentration product (or oxygen-induced EPR line broadening) across the thylakoid membrane at 20°C. Approximate locations of nitroxide fragments of spin labels are indicated by arrows. Data for aqueous phase (indicated by $\uparrow H_2O$) were obtained with 16-SASL, which at pH 9.5 is fairly soluble in water. Data points represent mean ± S.D. ($n = 4$).

nitroxide radicals increases with depth of location in the thylakoid membrane. This follows from Fig. 3, which demonstrates the dependence of the spin-label order parameter, S, calculated from spectral parameters $2T_{\parallel}'$ and $2T_{\perp}'$, on the position of the nitroxide radical in the stearic chain. The alkyl chain order is, however, surprisingly high to the depth of the twelfth carbon and decreases only at the depth of the 16th carbon. Alkyl chains of the lipid bilayer portion of the thylakoid membrane are very well ordered in the near polar headgroup region and fairly fluid in the membrane center. These characteristics suggest the possibility of lateral transport of non-polar molecules in the inner core region of the extended network of chloroplast membranes. Previously, Skulachev [43] noted the possibility of lateral transport of small hydrophobic solutes along the filamentous network of mitochondria.

4.2. Line broadening measurements of the oxygen diffusion–concentration product

The profile of the oxygen-induced line broadening of the central line of the EPR spectra from SASLs is shown in Fig. 4. Linewidth broadening increases with penetration of the nitroxide radical into the hydrophobic core of the thylakoid membrane, resulting in a maximal value in the central region of the membrane. Because of methodological difficulties, it was impossible to insert a nitroxide radical into the polar region of the thylakoid membrane. Therefore, we assumed that the oxygen diffusion–concentration product (and thus the $\Delta H_{pp}(x)$ value) changes linearly from the value at the 5-SASL position to the value for the aqueous phase obtained in a separate experiment from 16-SASL dissolved in water. Support for this assumption comes from the fact that for

Table 1
Oxygen permeability coefficient for thylakoid membranes at 20°C[a]

D_W^b (10^{-5} cm^2 s^{-1})	h^c (Å)	P_W (cm s^{-1})	P_m(EPR)/P_W(EPR)	P_m (cm s^{-1})
2.0	61.7	32.4	1.22	39.5

[a]Lipid composition of thylakoid membranes is extremely different from that of other intracellular organelles. The main components of thylakoid membrane polar lipids are uncharged galactolipids, MGDG and DGDG (see Fig. 1), which together account for about 70 mol% of total polar lipids in spinach thylakoids [54]. A very significant feature of thylakoid membranes is the high amount of polyunsaturated fatty acids. The main fatty acid is linolenic acid with three double bonds, C-18:3, which is more than 70 mol% of the total fatty acid of galactolipids [54–56].
[b]The bulk diffusion coefficient of oxygen in water [29].
[c]The thickness of the membrane is assumed to be the same as for the bilayer formed of the natural plant DGDG [57]. The thicknesses of the hydrocarbon layer and the polar headgroup region are 31.7 and 15 Å, respectively.

model membranes the oxygen diffusion–concentration product obtained with tempocholine dipalmitoylphosphatidic acid ester in the polar headgroup region lies between values for 5-SASL and SASL in the aqueous phase [18,44].

These results are also shown as the ratio of the local oxygen diffusion–concentration product in the membrane, $D(x)C(x)$, to that product in water, $D_W C_W$. The profile is very similar to those obtained for oxygen in unsaturated phosphatidylcholine membranes [18,19,44], but gives higher values of oxygen diffusion–concentration products than the profile across the Chinese hamster ovary plasma membrane [22]. Values of the oxygen diffusion–concentration product in thylakoid membranes equilibrated with 1 atm partial pressure of oxygen at 20°C can be obtained by multiplying the ratio of $D(x)C(x)/D_W C_W$ from Fig. 4 by the product $D_W C_W = 2.8 \times 10^{-11}$ mol cm^{-1} s^{-1} that was determined by classical diffusion measurement [29] and tables of oxygen solubility in water [45].

The oxygen diffusion–concentration product is itself significant because the rate of all chemical reactions involving oxygen depends on the collision frequency of oxygen with attacked molecules and thus, on the local oxygen diffusion–concentration product. In the membrane center, that product is about two times higher than in water, and chemical reactions such as lipid peroxidation and formation of active forms of oxygen can be expected to proceed more readily in the membrane center than in the hydrocarbon region close to the membrane surface.

4.3. Oxygen permeability across the thylakoid membrane

The permeability coefficient of the lipid bilayer portion of the thylakoid membrane, P_m(EPR), was

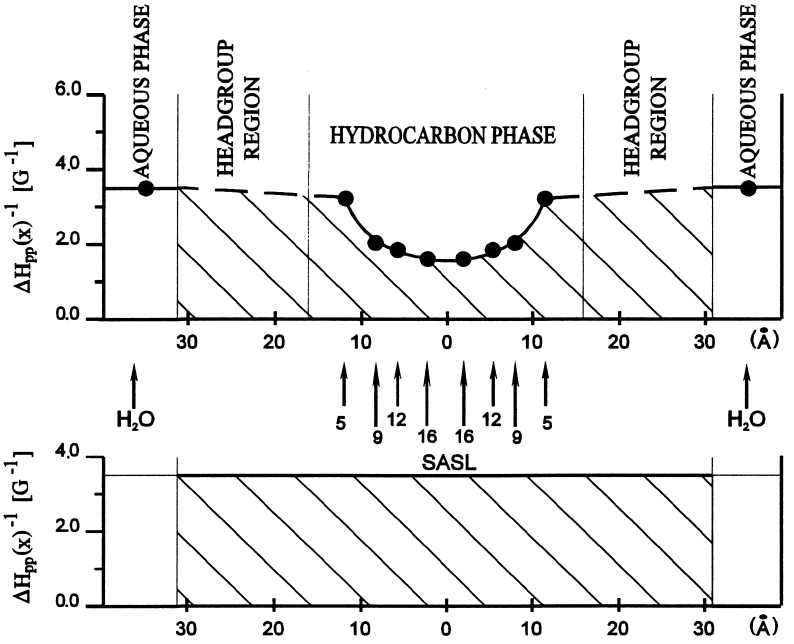

Fig. 5. Top: $(\Delta H_{pp}(x))^{-1}$ at 20°C is plotted as a function of the distance from the center of the thylakoid membrane to show the oxygen permeability barriers and the method of integration based on Eq. 4 (i.e. measuring the hatched area under the solid curve). The thickness of the membrane headgroup region and hydrocarbon region is assumed to be the same as for a bilayer formed of the natural plant galactolipids [57]. It is assumed that the locations of the alkyl chain carbon atoms in the membrane change linearly with the position on the alkyl chain [32] and that the nitroxide group of SASL is located at the mean depth of a certain carbon atom of the 1- and 2-chain of galactolipid. The average length of the alkyl chain is 18 carbons (see also Table 1, footnotes). Bottom: $(\Delta H_{pp}(\text{water}))^{-1}$ at 20°C plotted for a water layer of the same thickness as the membrane in order to illustrate the method of integration following Eq. 5 (measuring the hatched area under the solid line). The ratio of P_m(EPR)/P_W(EPR) is the ratio of the areas in the figures.

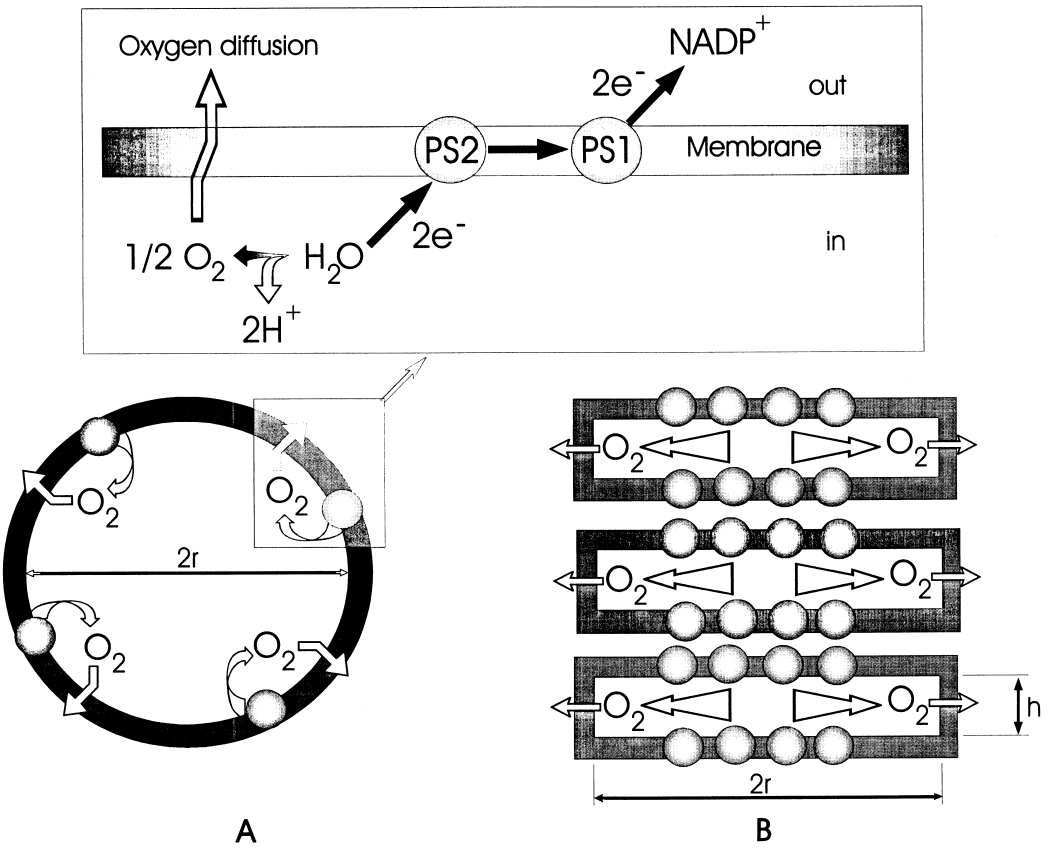

Fig. 6. Top: schematic representation of the non-cyclic electron transport in the thylakoid membrane and transmembrane diffusion of oxygen produced by the PS2 water-splitting complex. Bottom: schematic drawing of the thylakoid assuming a spherical shape (A) or as a disk-like vesicle (B). Dimensions used for calculation of the oxygen concentration difference across the thylakoid membrane are indicated.

evaluated using Eq. 4 with the integration performed based on Fig. 5, top. In this figure, the reciprocal value of oxygen-induced line broadening, $(\Delta H_{pp}(x))^{-1}$, is plotted as a function of distance from the membrane center. Integration is performed over the entire membrane thickness including the polar headgroup region, where we assume that $(\Delta H_{pp}(x))^{-1}$ changes linearly from the value of the 5-SASL position to the value obtained for the aqueous phase. The manner of integration of the oxygen permeability coefficient across a water layer of the same thickness as a membrane, P_W(EPR), is shown in Fig. 5, bottom. The ratio of P_m(EPR)/P_W(EPR) is the ratio of these two integrals: (dashed area shown in Fig. 5, bottom)/(dashed area shown in Fig. 5, top). As previously noted, by using the ratio of P_m(EPR)/P_W(EPR) the effect of uncertainty of the pR product from EPR measurements can be reduced. The final value of P_m is obtained by multiplying P_m(EPR)/P_W(EPR) by the permeability value of oxygen through the water layer of the same thickness as a membrane, as calculated from measurements of the bulk diffusion coefficient [29]. Data are shown in Table 1. Table 1 contains the information used for the evaluation of the membrane thickness. These data indicate that the lipid bilayer portion of the thylakoid membrane does not retard oxygen diffusion from the thylakoid. This lipid bilayer portion is not a barrier to oxygen permeation because $P_m/P_W > 1$.

4.4. Oxygen concentration difference across the thylakoid membrane

The knowledge of the membrane oxygen permeability coefficient, P_m, and the rate of oxygen production by functioning chloroplasts, J, permits calculation of the possible oxygen concentration

difference across the membrane, ΔC, from the phenomenological relationship $J = P_m \Delta C$. In the case of the non-cyclic electron transport, a transmembrane oxygen flux can be evaluated as $J = NV/S$, where N is a number of oxygen-producing PS2 complexes per one thylakoid, V is a rate of oxygen production by one PS2 complex, and S is an efficient surface of a thylakoid that is permeable for oxygen. It is reasonable to take $N = 1000$ and $V = 100\ s^{-1}$ [46]. Considering a thylakoid as the oxygen-transparent sphere of radius $r \approx 1000$ Å (Fig. 6A), $\Delta C \approx 3.3$ nM is obtained. However, under normal physiological conditions, thylakoids of grana, which contain water-splitting complexes, represent appressed disk-like vesicles. In this case, oxygen diffusion should proceed predominantly through the rather narrow side surface of the disk which is exposed to stroma. Taking the radius of the disk $r \approx 1000$ Å and height $h \approx 100$ Å (Fig. 6B), $\Delta C \approx 0.1$ μM is obtained. The top portion of Fig. 6 shows a scheme for the non-cyclic electron transport in the thylakoid membrane and transmembrane diffusion of oxygen produced by the PS2 water-splitting complex.

Data do exist indicating that protein content in the membrane can affect the oxygen permeability coefficient [47,48]. These studies, however, introduce another level of complication: they demonstrate variation of oxygen transport between bulk lipids and boundary layers of proteins, between protein clusters and bulk lipids, between lipid domains, and within the integral membrane protein itself. Thylakoid membranes belong to a group of protein-rich membranes with a typical protein-to-lipid ratio (w/w) of 1.5 [49]. Because integral membrane proteins [47,50] as well as water-soluble proteins [51,52] are impermeable to oxygen, the oxygen concentration difference can be increased several times (by a factor proportional to the ratio of the surface area of thylakoid to the surface area of its lipid bilayer portion). With these corrections it can still be concluded that the oxygen concentration difference across the thylakoid membrane generated under the illumination of the leaf should be negligible (less than 1 μM).

In our previous work [10,53], we measured the kinetics of light-induced oxygenation of the interior of a bean leaf using either a specially prepared microscopic water-soluble probe for oxygen (serum albumin-coated paraffin oil particles containing cholestane spin label) or paramagnetic fusinite particles. In the former experiment [10], it was demonstrated that the intense actinic light induced only a very small net increase (less than 2.5%) in oxygen concentration in the bulk of aqueous phase of the leaf interior. However, results of the latter experiment [53] did not show any significant changes in the oxygen level. These measurements were performed 24 h after fusinite injection into a bean leaf, so the excess water injected into the intercellular compartments of the leaf had time to evaporate. The experiment indicated a fast diffusion of oxygen from the leaf, i.e., a good ventilation of its interior. Results of our measurements in the present study demonstrate that high permeability of a thylakoid membrane for oxygen should preclude any significant increase in the concentration of oxygen in local chloroplast compartments ($\Delta C \leq 1$ μM). Thus, we conclude that photosynthetic production of oxygen in itself should not be damaging to the thylakoid membrane.

This conclusion, of course, does not mean that the functioning of photosynthetic apparatus of chloroplast would not produce toxic forms of oxygen (superoxide radicals, hydrogen peroxide) that can arise due to oxygen interaction with the reduced electron transport carriers. One might expect an increased steady-state yield of toxic forms of oxygen because of a light-induced increase in oxygen concentration. However, the high permeability of thylakoid membranes to oxygen and the good ventilation of the leaf interior [10,53] will mediate the increase of oxygen concentration and thus diminish the production of dangerous active forms of oxygen.

Acknowledgements

This work was supported in part by grants GM22923 and RR01008 from the US National Institutes of Health and Grant 97-04-49554 from the Russian Foundation for Basic Research. Partial support from Jagiellonian University is appreciated.

References

[1] A.N. Mehler, Arch. Biochem. Biophys. 33 (1951) 65–77.
[2] U. Heber, U. Egneus, M. Jensen, S. Koster, Planta 143 (1978) 41–49.

[3] J. Harbinson, B. Genty, N.R. Baker, Photosynth. Res. 25 (1990) 213–224.
[4] G. Edwards, D.A. Walker, C_3, C_4: Mechanisms, and Cellular and Environmental Regulation of Photosynthesis, Blackwell, Oxford, 1983.
[5] D. Arnon, R.K. Chain, FEBS Lett. 82 (1977) 297–302.
[6] R.E. Slovacek, G. Hind, Plant Physiol. 60 (1977) 538–542.
[7] R. Malkin, R.K. Chain, Biochim. Biophys. Acta 591 (1980) 381–390.
[8] K.S.R. Chapman, J.A. Berry, M.D. Hatch, Arch. Biochem. Biophys. 202 (1980) 330–341.
[9] M.K. Solntzev, A.N. Tikhonov, in: Environmental Factors and Primary Photosynthetic Processes (in Russian), Naukova Dumka, Kiev, 1989, pp. 117–120.
[10] A. Ligeza, A. Wisniewska, K. Subczynski, A.N. Tikhonov, Biochim. Biophys. Acta 1186 (1994) 201–208.
[11] S. Riistama, A. Puustinen, A. García-Horsoman, S. Iwata, H. Michel, M. Wikström, Biochim. Biophys. Acta 1275 (1996) 1–4.
[12] S. Belkin, R.J. Mehlhorn, L. Packer, Arch. Biochem. Biophys. 252 (1987) 487–495.
[13] D.I. Kyle, in: D.I. Kyle, C.B. Osmond, C.J. Arutzen (Eds.), Topics in Photosynthesis, Vol. 9, Elsevier, Amsterdam, 1987, pp. 197–226.
[14] I. Vass, S. Styring, T. Hundal, A. Koivuniemi, E.-M. Aro, B. Andersson, Proc. Natl. Acad. Sci. USA 89 (1992) 1408–1412.
[15] E.-M. Aro, I. Virgin, B. Andersson, Biochim. Biophys. Acta 1143 (1993) 113–134.
[16] K.J. Liu, P. Gast, M. Moussavi, S.W. Norby, N. Vahidi, T. Walczak, M. Wu, H.M. Swartz, Proc. Natl. Acad. Sci. USA 90 (1993) 5438–5442.
[17] H.M. Swartz, S. Boyer, P. Gast, J.F. Glockner, H. Hu, K.J. Liu, M. Moussavi, S.W. Norby, N. Vahidi, T. Walczak, M. Wu, R.B. Clarkson, Magn. Reson. Med. 20 (1991) 333–339.
[18] W.K. Subczynski, J.S. Hyde, A. Kusumi, Proc. Natl. Acad. Sci. USA 86 (1989) 4474–4478.
[19] W.K. Subczynski, E. Markowska, Curr. Top. Biophys. 16 (1992) 62–68.
[20] W.K. Subczynski, J.S. Hyde, Biophys. J. 45 (1984) 743–748.
[21] J.S. Hyde, W.K. Subczynski, J. Magn. Reson. 56 (1984) 125–130.
[22] W.K. Subczynski, L.E. Hopwood, J.S. Hyde, J. Gen. Physiol. 100 (1992) 68–87.
[23] J.S. Hyde, W.K. Subczynski, in: L.J. Berliner, J. Reuben (Eds.), Biological Magnetic Resonance, Vol. 8, Spin Labeling: Theory and Applications, Plenum, New York, 1989, pp. 399–425.
[24] D.A. Windrem, W.Z. Plachy, Biochim. Biophys. Acta 600 (1980) 655–665.
[25] M.P. Eastman, R.G. Kosser, M.R. Das, J.H. Freed, J. Chem. Phys. 51 (1969) 2690–2709.
[26] J.C. Lang, J.H. Freed, J. Chem. Phys. 56 (1972) 4103–4114.
[27] S. Fischkoff, J.M. Vanderkooi, J. Gen. Physiol. 65 (1975) 663–676.
[28] C.A. Popp, J.S. Hyde, Proc. Natl. Acad. Sci. USA 79 (1982) 2559–2563.
[29] C.E. St. Denis, C.J. Fell, Can. J. Chem. Eng. 49 (1971) 885.
[30] Y.N. Molin, K.M. Salikhov, K.I. Zamaraev, Spin Exchange, Springer, New York, 1980, pp. 111–115.
[31] J.-J. Yin, J.B. Feix, J.S. Hyde, Biophys. J. 58 (1990) 713–720.
[32] G. Zaccai, G. Buldt, A. Seelig, J. Seelig, J. Mol. Biol. 134 (1979) 693–706.
[33] J.M. Diamond, Y. Katz, J. Membr. Biol. 17 (1974) 121–154.
[34] A. Kusumi, W.K. Subczynski, J.S. Hyde, Proc. Natl. Acad. Sci. USA 79 (1982) 1854–1858.
[35] M. Pasenkiewicz-Gierula, W.K. Subczynski, Curr. Top. Biophys. 20 (1996) 93–98.
[36] S.-J. Marrink, H.J.C. Berendsen, J. Phys. Chem. 98 (1994) 4155–4168.
[37] J.S. Stamler, D.J. Singel, J. Loscalzo, Science 258 (1992) 1898–1902.
[38] M. Lomnicka, W.K. Subczynski, Curr. Top. Biophys. 20 (1996) 76–80.
[39] K. Strzalka, T. Sarna, J.S. Hyde, Photobiochem. Photobiophys. 12 (1986) 67–71.
[40] D.O. Nettelton, P.D. Morse II, J.W. Dobrucki, H.M. Swartz, N.J.F. Dodd, Biochim. Biophys. Acta 944 (1988) 315–320.
[41] F. Kamp, D. Zakim, N. Noy, J.A. Hamilton, Biochemistry 34 (1995) 11928–11937.
[42] J.F.W. Keana, S. Pou, Physiol. Chem. Phys. Med. NMR 17 (1985) 235–240.
[43] V.P. Skulachev, J. Membr. Biol. 114 (1990) 97–112.
[44] W.K. Subczynski, J.S. Hyde, A. Kusumi, Biochemistry 30 (1991) 8578–8590.
[45] M.L. Hitchman, Measurement of Dissolved Oxygen, Wiley, New York, 1978.
[46] H. Witt, Biochim. Biophys. Acta 505 (1979) 355–427.
[47] C. Altenbach, T. Marti, H.G. Khorana, W.L. Hubbell, Science 248 (1990) 1088–1092.
[48] I. Ashikawa, J.-J. Yin, W.K. Subczynski, T. Kouyama, J.S. Hyde, A. Kusumi, Biochemistry 33 (1994) 4947–4952.
[49] P.J. Quinn, W.P. Williams, Biochim. Biophys. Acta 737 (1983) 223–266.
[50] W.K. Subczynski, G. Renk, R. Crouch, J.S. Hyde, A. Kusumi, Biophys. J. 63 (1992) 573–577.
[51] D.B. Calhoun, S.W. Englander, W.W. Wright, J.M. Vanderkooi, Biochemistry 27 (1988) 8466–8474.
[52] J.E. Brunet, C. Jullian, D.M. Jameson, Photochem. Photobiol. 51 (1990) 487–489.
[53] A. Ligeza, A.N. Tikhonov, W.K. Subczynski, Biochim. Biophys. Acta 1319 (1997) 133–137.
[54] M. Nishihara, K. Yokota, M. Kito, Biochim. Biophys. Acta 617 (1980) 12–19.
[55] J.M. Anderson, Biochim. Biophys. Acta 416 (1975) 191–235.
[56] T. Guillot-Salomon, J. Bahl, L. Ben-Rais, M.-J. Alpha, C. Cantrel, J.-P. Dubacq, Plant Physiol. Biochem. 29 (1991) 667–679.
[57] W.I. Gruszecki, J. Sielewiesiuk, Biochim. Biophys. Acta 1069 (1991) 21–26.